Available online at www.sciencedirect.com
ScienceDirect
Carbohydrate Research 342 (2007) 1613–1623
Carbohydrate RESEARCH

Minireview

# Dissecting the catalytic mechanism of a plant β-D-glucan glucohydrolase through structural biology using inhibitors and substrate analogues

Maria Hrmova* and Geoffrey B. Fincher

*Australian Centre for Plant Functional Genomics, School of Agriculture, Food and Wine, University of Adelaide, Waite Campus, Glen Osmond, SA 5064, Australia*

Received 23 March 2007; received in revised form 4 May 2007; accepted 8 May 2007
Available online 18 May 2007

**Abstract**—Higher plant, family GH3 β-D-glucan glucohydrolases exhibit *exo*-hydrolytic and retaining (e→e) mechanisms of action and catalyze the removal of single glucosyl residues from the non-reducing termini of β-D-linked glucosidic substrates, with retention of anomeric configuration. The broad specificity β-D-glucan glucohydrolases are likely to play roles in cell wall re-modelling, turnover of cell wall components and possibly in plant defence reactions against pathogens. Crystal structures of the barley β-D-glucan glucohydrolase, obtained from both native enzyme and from the enzyme in complex with a substrate analogues and mechanism-based inhibitors, have enabled the basis of substrate specificity, the mechanism of catalysis, and the role of domain movements during the catalytic cycle to be defined in precise molecular terms. The active site of the enzyme forms a shallow 'pocket' that is located at the interface of two domains of the enzyme and accommodates two glucosyl residues. The propensity of the enzyme to hydrolyze a broad range of substrates with (1→2)-, (1→3)-, (1→4)- and (1→6)-β-D-glucosidic linkages is explained from crystal structures of the enzyme in complex with non-hydrolysable S-glycoside substrate analogues, and from molecular modelling. During binding of gluco-oligosaccharides, the glucosyl residue at subsite −1 is locked in a highly constrained position, but the glucosyl residue at the +1 subsite is free to adjust its position between two tryptophan residues positioned at the entry of the active site pocket. The flexibility at subsite +1 and the projection of the remainder of the substrate away from the pocket provide a structural rationale for the capacity of the enzyme to accommodate and hydrolyze glucosides with different linkage positions and hence different overall conformations. While mechanism-based inhibitors with micromolar $K_i$ constants bind in the active site of the enzyme and form esters with the catalytic nucleophile, transition-state mimics bind with their 'glucose' moieties distorted into the $^4E$ conformation, which is critical for the nanomolar binding of these inhibitors to the enzyme. The glucose product of the reaction, which is released from the non-reducing termini of substrates, remains bound to the β-D-glucan glucohydrolase in the −1 subsite of the active site, until a new substrate molecule approaches the enzyme. If dissociation of the glucose from the enzyme active site could be synchronized throughout the crystal, time-resolved Laue X-ray crystallography could be used to follow the conformational changes that occur as the glucose product diffuses away and the incoming substrate is bound by the enzyme.


*Keywords:* Conventional and time-resolved Laue X-ray crystallography; Domain movements; Mechanism-based Inhibitors; Substrate analogues; Transition-state mimics

**Contents**



* Corresponding author. Tel.: +61 8 8303 7280; fax: +61 8 8303 7102; e-mail: maria.hrmova@adelaide.edu.au

0008-6215/$ - see front matter © 2007 Elsevier Ltd. All rights reserved.
doi:10.1016/j.carres.2007.05.013

## 1. Introduction

Glycoside hydrolases constitute a widely distributed group of enzymes that play key roles in a broad spectrum of biological processes. They have been divided into 110 separate families and 14 clans (http://www.cazy.org/).[1] These divisions are based on differences in primary, secondary and three-dimensional structures of the enzymes; the latter can be defined by about seven different protein folds.

The aim of this review is to illustrate how structural biology, combined with information on the effects of substrate analogues and inhibitors, can be applied to define the molecular details of enzyme specificity and catalysis, and hence to define structure–function relationship of particular enzymes. A higher plant β-D-glucan glucohydrolase that is classified in the family GH3 group of enzymes is used as a paradigm for this analysis. The structural approach clearly requires that the enzyme under investigation can be crystallized and further requires an array of specifically designed low-molecular mass substrate analogues and inhibitors.

Barley β-D-glucan glucohydrolases belong to the GH3 family of glycoside hydrolases, according to the Carbohydrate-Active enZymes (CAZy) classification (http://www.cazy.org/); the GH3 family includes approximately 1200 entries from the GenBank/GenPept databases.[1] The latter entries are predominantly nucleotide sequences from genome sequencing programs, and in the vast majority of cases their substrate specificities and functions have not been tested. More than 200 enzymes are classified in the GH3 family. Almost all members have two, three or more individually folded domains,[2,3] although the sequential arrangement of the domains can vary. The enzymes are variously annotated as β-D-glucosidases, (1→3;1→4)- and (1→3)-β-D-glucan *exo*-hydrolases, β-D-xylosidases, α-L-arabinofuranosidases and *N*-acetyl β-D-glucosaminidases.[1,2] As mentioned above, the substrate specificities assigned to the GH3 family members have been based mainly on similarities between nucleotide sequences of the genes with a small number of enzymes for which biochemical data are available, and thus the substrate specificity annotations can be unreliable.

The GH3 family members are distributed mainly in eubacteria, fungi and plants, and are rare or absent in Archaea and animals.[1,2,4] Phylogenetic analyses of the GH3 family indicate that it is one of three families (the others are GH13 and GH23) that are highly represented in bacterial genomes.[4] However, the broad distribution of family GH3 members in various kingdoms suggests that they play key roles in numerous fundamental biological processes. Some of these functions include the microbial degradation of plant residues, the modification of structures of glycosides, bacterial antibiotics and plant-derived antifungal molecules, the turn-over, recycling and remodelling of cellular components in bacteria, fungi and plants, and the modification of host–pathogen interactions during the microbial infection of plants.[4,5] For example, in plants, lily and maize *exo*-β-D-glucanases play roles in pollen development,[6] while in barley seedlings the orthologous β-D-glucan glucohydrolases are believed to participate in hydrolysis of cell wall poly- and oligosaccharides.[6–9]

A great deal of attention has been focused upon the biochemical and structural characterization of the barley β-D-glucan glucohydrolases.[7,8] Two β-D-glucan glucohydrolases, designated isoenzymes ExoI and ExoII, were purified to near homogeneity from germinated barley seedlings,[7] and the complete amino acid sequences of the two isoforms have been deduced from the corresponding cDNAs (GenBank™/EMBL Data Bank accession numbers for isoenzymes ExoI and ExoII are AF102868 and U46003, respectively).[7,9] Additional isoforms have been detected in barley[10,11] and the enzymes are also abundant in maize coleoptiles[12] and dicotyledonous plants.[13,14] The β-D-glucan glucohydrolase isoenzymes ExoI and ExoII have broad substrate specificities. They hydrolyze unbranched and unsubstituted β-D-glucans such as (1→3)-β-D-glucans and (1→3;1→4)-β-D-glucans;[15] the latter substrate represents an important component of cell walls in the Poaceae family of higher plants, while the former are abundant in fungal cell walls. Further, the two barley β-D-glucan glucohydrolases hydrolyze β-D-gluco-oligosaccharides with (1→2)-, (1→3)-, (1→4)- or (1→6)-linked sugar moieties, as well as aryl β-D-glucosides such as 4-nitrophenyl β-D-glucoside.[15] The enzymes remove single glucose units from the non-reducing termini of polymeric and oligomeric substrates, with retention of anomeric configuration.[7,15] As typical retaining hydrolases,[7] the barley β-D-glucan glucohydrolases[15,16] and other GH3 family β-D-glucosidases[17–19] exhibit transglycosylation activity at high substrate concentrations, and the higher molecular mass glucosyl transfer products that are formed in these reactions are usually (1→6)-linked, but (1→3)- and (1→4)-linked transglycosylation products can also be formed, albeit in lower yields.[15–19] The transglycosylation activity of these hydrolases can be considered as a mechanistic consequence of a kineti-

cally controlled reaction, in which the natural reaction equilibrium with water is displaced through an excess of glucoside acceptor molecules.[20] These mechanistic transglycosylation reactions are unlikely to be of biological significance.

Because the barley β-D-glucan glucohydrolases exhibit a broad substrate specificity, they are difficult to classify in existing Enzyme Commission classes.[7,8] However, they are fundamentally different from the previously characterized β-D-glucosidases from families GH1[1,21,22] and GH9[1] or from the cellobiohydrolases of families GH6, GH7, GH9, GH10, GH48 and GH74.[1,23,24]

## 2. The three-dimensional structure of barley β-D-glucan glucohydrolase

The barley β-D-glucan glucohydrolase isoenzyme ExoI can be purified from seedlings in relatively good yields, which makes it a suitable target for protein crystallography.[7,25] Once in a mono-disperse form, the enzyme readily crystallizes in a $P4_32_12$ tetragonal space group and numerous crystals resolving at better than 1.60 Å can be obtained;[25] in the crystals the enzyme remains in the active form.[25] The crystals can be of exceptional quality and exhibit a low mosaic spread, and this allows diffusion of a mechanism-based inhibitor, transition-state mimics and non-hydrolyzable substrate analogues into the crystals. The ligand–enzyme complexes provide an opportunity to identify specific amino acid residues that are involved in substrate binding and catalysis, and to define in detail the mechanism of hydrolysis of the glycosidic linkages.[8,16,26,27] This approach ultimately results in defining the molecular basis for substrate binding, substrate specificity, mechanisms of catalysis and, through molecular modelling, the structural data allow evolutionary relationships amongst β-D-glucan glucohydrolases and other GH3 family members to be unraveled.[1,2,4]

Lastly, molecular events associated with trafficking of incoming substrate molecules and the dissociation of the product of the previous catalytic event can be investigated in native crystals, given that the glucose product of the reaction remains bound in the active site of the purified enzyme.[26,27] To this end, the mono-disperse quality of the β-D-glucan glucohydrolase protein isolated barley seedlings offers some advantages over an enzyme expressed in heterologous hosts, including native post-translational modification patterns and an enzyme, in which a glucose molecule is caught in the active site.

The first crystal structure of the native barley β-D-glucan glucohydrolase isoenzyme ExoI was determined by X-ray crystallography using multiple isomorphous replacement technique to 2.20 Å resolution,[26] and represented the first three-dimensional (3D) structure for a GH3 enzyme; Protein Data Bank (PDB) entries 1EX1[26] and 1IEQ.[27] Indeed, the β-D-glucan glucohydrolase structure remains the only completely solved 3D structure in the GH3 family of glycoside hydrolases,[26,27] although the structure of the $(\alpha/\beta)_8$ TIM barrel domain 1 of an *N*-acetyl-β-glucosaminidase from *Vibrio cholerae* has recently been reported in its free form and in complex with *N*-acetyl-β-D-glucosamine (GlcNAc) (PDB entries 1TR9 and 1Y65; J. Gorman and L. Shapiro, New York Structural Genomics Research). In this context, crystals of β-D-glucosidase from *Thermotoga neapolitana* and *Septoria lycopersici*, β-*N*-acetylhexosaminidase from *Thermotoga maritima*, and β-D-xylosidase from *Vibrio cholerae* and *Hypocrea jecorina* have been reported, but the 3D structures of respective proteins have not yet been published.[1]

The β-D-glucan glucohydrolase enzyme adopts a globular, two domain modular structure.[26] The first 357 amino acid residues represent the first domain and fold into an $(\alpha/\beta)_8$ TIM-barrel conformation. This $NH_2$-terminal domain is joined by a 16 amino acid helix-like linker to the second domain, which consists of residues 374–559 and which forms a six-stranded β-sheet flanked on either side by three α-helices; this second domain therefore constitutes an $(\alpha/\beta)_6$ sandwich (Fig. 1). An antiparallel loop of 42 amino acid residues is located at the COOH-terminus of the enzyme (Fig. 1). This loop is highly conserved across most of the GH3 family.[2] A pocket about 13 Å in depth at the interface of the two domains has been identified as the active site of the enzyme. The dimensions of the pocket indicate that it could accommodate two glucosyl residues;[16,26,27] this is compatible with subsite mapping data.[16] The enzyme binds the various substrates at their non-reducing ends, and the restricted depth of the dead-end pocket, coupled with the relative disposition of the catalytic amino acid residues, ensures that only the last glycosidic linkage at the non-reducing end of the substrate can be hydrolyzed. Thus, the exo-action pattern of the enzyme can be explained in structural terms. The shape of the active site in the barley β-D-glucan glucohydrolase can be contrasted with those of endo-hydrolases, which usually have open cleft- or tunnel-like topologies that allow random binding of the enzyme to internal regions of polysaccharide substrates.[1,6,28]

The structural analysis of the purified and crystallized barley β-D-glucan glucohydrolase revealed that a glucose molecule is bound in the active site pocket of the enzyme (Fig. 1). The glucose is presumed to be the product of the enzyme-catalyzed reaction that has not been released after hydrolysis is completed.[26,27] It is remarkable that this glucose molecule remains bound to the −1 subsite of the active site pocket, even after protracted protein purification procedures that include ion-exchange, hydrophobic and size-exclusion chromatography and chromatofocussing,[7] and after crystallization for several months. Glucose occupancy in the crystals

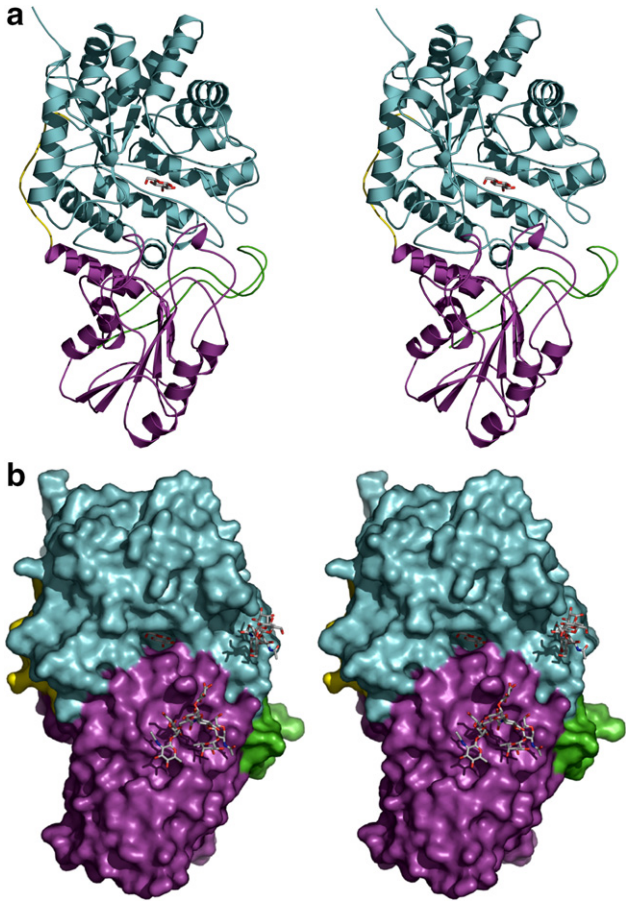


**Figure 1.** (a) A representation of native β-D-glucan glucohydrolase with bound glucose (in cpk colours), where domain 1 (residues 1–357), linker (358–373), domain 2 (374–559) and the COOH-terminal antiparallel loop (560–602) are in cyan, yellow, magenta and green, respectively. (b) Molecular surface drawing of native β-D-glucan glucohydrolase (colours as specified in panel a) with two occupied Asn221 and Asn498-linked glycosylation sites (cpk colours). Adapted with permission from Elsevier Science.[27]

is approximately one. The dissociation constant for the glucose–enzyme complex ($K_i$) has been calculated at approximately 9 mM, using 4-nitrophenyl β-D-glucoside as the substrate,[7] but this value presumably does not reflect the strength of binding of the glucose product to the enzyme following hydrolysis. We have not yet measured the dissociation constant $K_d$ (off-rate constant) for glucose, which could be determined by pre-steady-state kinetic analyses. Nevertheless, the crystallized enzyme with the bound glucose product represents a rare opportunity to study the structural events that occur, when the bound product is eventually displaced as the incoming substrate molecule approaches the active site.[16,26,27]

An emerging and fascinating technique for monitoring product–substrate trafficking in the active sites of enzymes is time-resolved Laue X-ray crystallography or four-dimensional crystallography.[29,30] The successful deployment of this procedure requires the coordinated and simultaneous dissociation of ligand molecules from the active sites of all enzyme molecules in the crystal. Thus, if we could synchronize dissociation of glucose from the enzyme active site throughout the crystal, the time-resolved Laue crystallography could be used to monitor, in real time, the product diffusing away from the enzyme's pocket.[29,30]

Another unexpected opportunity afforded by the binding of the glucose product to the barley β-D-glucan glucohydrolase was that details of amino acid residue interactions with the glucose bound at subsite −1 of the active site could be defined in exact atomic terms.[26,27] About 12 amino acid residues contribute to binding of this single glucose molecule, from which six amino acid residues participate in hydrogen bonds with OH groups of glucose at the separations of 2.52–2.96 Å. This not only demonstrates the complexity and 3D perfection of the chemical and geometrical complementarity of substrate binding and specificity, but it also offers an explanation for the apparently tight binding of the glucose that remains in the active site during purification and crystallization.

Last but not least, the availability of the crystal structure of the barley β-D-glucan glucohydrolase proved useful for comparative protein modelling, through which reliable models of other members of the GH3 family could be constructed and potential differences in substrate specificity could be identified.[1,2,4,8] However, comparative modelling should be applied and interpreted with caution when sequence identities between templates and targets fall within the 'twilight zones' of around 20% or less. For example, the structural data of the barley β-D-glucan glucohydrolase are not likely to be useful for rationalizing differences in substrate specificity between the family GH3 β-D-glucan glucohydrolases[7] and β-D-xylosidases.[31] Members of the plant β-D-xylosidase-like group of enzymes in family GH3 also have α-L-arabinofuranosidase activity[31] and this might further complicate substrate specificity assignments. Hence, the structural information for barley β-D-glucan glucohydrolase might be useful for closely related enzymes, but cannot be satisfyingly applied to more distantly related enzymes such as the plant β-D-xylosidases. This limitation clearly applies more broadly to hydrolytic enzymes that are grouped into the same family and an important requirement for glycosyl hydrolases classification in general is to isolate and characterize the substrate preferences of representative enzymes from individual sub-families (Henrissat, B., personal communication). Similarly, new crystal structures of plant and other enzymes within subfamilies of the GH3 group are urgently needed. Nevertheless, careful analysis of sequences encoding substrate binding regions might allow the discrimination of family GH3 β-D-glucosidases, (1→3;1→4)- and (1→3)-β-D-glucan *exo*-hydrolases, and β-D-xylosidases and α-L-arabinofuranosidases. These considerations are of particular

relevance for the annotation of cereal and other plant genomes, where structural comparisons might ultimately assist in defining functions of unknown genes and/or in defining the effects of nucleotide polymorphisms and allelic variation.

## 3. Basis of substrate specificity

To describe the binding interactions between substrates and amino acid residues on the enzyme's surface, and thus to dissect the basis of substrate specificity of the barley β-D-glucan glucohydrolase, two non-hydrolysable S-glycoside substrate analogues $4^{I}$, $4^{III}$, $4^{V}$-S-trithiocellohexaose[27] (PDB accession code 1IEX) and 4′-nitrophenyl *S*-β-D-glucopyranosyl-(1→3)-3-thio-β-D-glucopyranosyl-(1→3)-β-D-glucopyranoside (PDB accession code 1J8V), were synthesized and soaked into enzyme crystals.[16] The 3D structures of the thio-analogue–enzyme complexes demonstrated that both ligands displaced the glucose molecule that is normally bound in the active site pocket of the enzyme, and that the two non-reducing end residues of the inhibitors are positioned in the pocket at the −1 and +1 subsites (Fig. 2). While the glucosyl residue at subsite −1 is tightly constrained through extensive hydrogen bonding with multiple amino acid residues, the glucosyl residue at subsite +1 is sandwiched between large tryptophan residues (Trp286 and Trp434). The hydrophobic interactions between the glucosyl residue at subsite +1 and the tryptophan residues are not as precise as the multiple hydrogen bonding interactions at subsite −1, and hence the glucosyl residue at subsite +1 is not so tightly constrained (Fig. 2). As a result, differences in the spatial positions of non-reducing and penultimate glucosyl residues in say (1→3)- and (1→4)-β-D-linked glucoside substrates can be accommodated through the flexibility of binding at the +1 subsite. Moreover, the active site pocket is only deep enough to bind two glucosyl residues, so that the remainder of polymeric substrates must project away from the active site pocket, without making contact with the enzyme surface.[16,27] Again, one would anticipate that the overall conformation of β-D-polyglucosyl substrates, which would ultimately be defined by linkage types between the β-D-glucosyl residues, would not greatly affect the ability of the enzyme to bind the two non-reducing residues. This would explain the broad specificity of these enzymes with respect to their ability to hydrolyze substrates with (1→2)-, (1→3)-, (1→4)- and (1→6)-β-D-glucosidic linkages.[16,27] Nevertheless, more direct evidence was required to support this possibility, as described below.

Crystallographic analyses indicate that only minor distortions of the glucopyranosyl ring of the S-cellobioside and S-laminaribioside moieties at subsite −1 occur, and the sugar rings at both subsites can therefore be modelled in the $^{4}C_{1}$ low-energy conformation[16,27] (Figs. 2 and 3). When the planes defined by the sugar ring atoms of the bound S-cellobioside moiety and of a free cellobiose molecule are superposed, the C1–S(O)–C4′–C3′ dihedral angles of both sugars differ by approximately 10°.[27] Similarly, the glucopyranosyl residue of the S-laminaribioside moiety at subsite −1 and free laminaribiose diverged by approximately 50°.[16] These analyses suggested that the sugar rings in the bound S-cellobioside or S-laminaribioside moieties at the −1 subsite are only marginally translated and tilted around their glycosidic linkages. However, at the relatively low resolution of the X-ray data (2.20–2.40 Å), the possibility of small distortions in the ring conformation at the −1 subsites cannot be discounted. Thus, requirements for

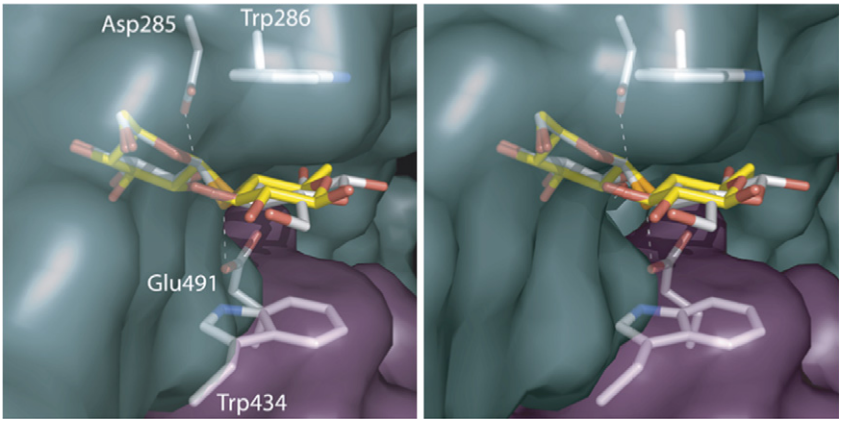


**Figure 2.** Stereo representation of the active site of barley β-D-glucan glucohydrolase with bound S-cellobioside and S-laminaribioside moieties. The S-cellobioside and S-laminaribioside moieties are presented as sticks and atoms are coloured grey (carbons; yellow for S-laminaribioside), orange (sulfur) and red (oxygens). Transparent cyan and magenta colours represent the molecular surfaces of domains 1 and 2, respectively. The structures were superposed over the $C^{\alpha}$ atoms of 14 active site amino acid residues, with a rmsd in the $C^{\alpha}$ chain positions of 0.158 Å. To improve clarity of the diagrams, selected amino acid residues Asp285, Trp286, Trp434 and Glu491 are shown (grey, red and blue represent carbons, nitrogens and oxygens). The entrance to the active site is located towards the lower right hand corner. Adapted with permission from the American Society of Plant Biologists.[16]

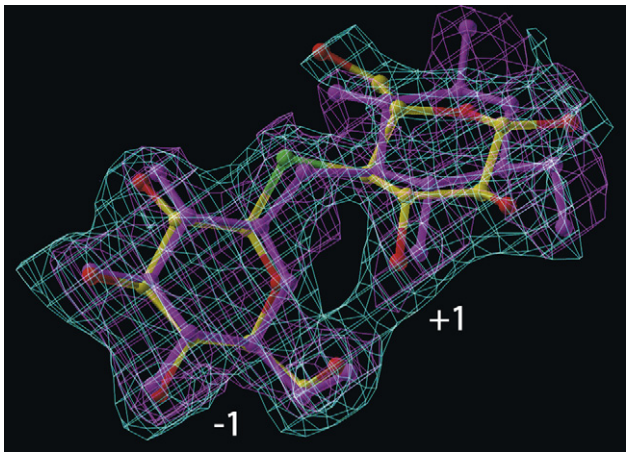


**Figure 3.** The electron density map of the S-laminaribioside moiety superposed over the −1 subsite of the S-cellobioside moiety in the active site of the barley β-D-glucan glucohydrolase. The derived $2|F_o| - |F_c|$ and $|F_o| - |F_c|$ Fourier syntheses are contoured at 1.0σ and 1.15σ for the S-cellobioside and the S-laminaribioside moieties, respectively. The S-cellobioside moiety is represented in atom colours and its associated electron density map is coloured green, while the S-laminaribioside atoms and the associated electron density map are coloured magenta. Adapted with permission from the American Society of Plant Biologists.[16]

distortion/relaxation of the glucopyranosyl moiety in the active site seem to be limited, although significant ring distortions at subsite −1 have been observed by other groups in several inhibitor–glycoside hydrolase complexes.[32–36]

The possible binding conformations of the two remaining positional isomers of β-D-diglucosides, namely those of the (1→2)-linked disaccharide sophorose and the (1→6)-linked disaccharide gentiobiose, were investigated by molecular modelling, based on the crystal structures of sophorose[16,37] and gentiobiose[16,38] and the 3D structure of the barley β-D-glucan glucohydrolase.[26] It is envisaged that these oligosaccharides are held in place by almost exactly the same amino acid residues as the S-laminaribioside– and S-cellobioside–enzyme complexes. As for the orientations of the sugar moieties, for sophorose, the polar face of the glucopyranosyl ring at subsite +1 is superposed with the pyrrole region of Trp286, while its apolar face is superposed with the phenyl region of Trp434. Gentiobiose adopts a position that is similar to the position of S-laminaribioside moiety. During molecular modelling of gentiobiose–enzyme interactions, the extra rotatable bond C6′–C5′ that connects the two glucopyranosyl rings in gentiobiose resulted in the displacement of the glucopyranosyl ring from the boundary outlined by the two Trp residues at subsite +1. However, further crystallographic evidence for 4′-nitrophenyl gentiobioside–enzyme and 1-*O*-methyl-thio-gentiobioside (G6sG-OMe)–enzyme complexes indicated that the glucopyranosyl ring of the gentiobioside moiety is indeed aligned between the pyrrole/phenyl rings of Trp286 and Trp434 (Hrmova, M.; Fort, S.; Driguez, H.; Varghese, J. N.; Fincher, G. B., unpublished data), presumably because of the flexibility of the C6′–C5′ rotatable bond that connects the glucopyranosyl rings in gentiobiose.

From the superpositions of the S-laminaribioside– and the S-cellobioside–enzyme complexes, and from the sophorose- and gentiobiose–enzyme models, it is possible to come up with a structural rationale for a broad substrate specificity of the enzyme. For all ligand–enzyme structures, the glucopyranosyl residues at −1 subsites are bound in almost identical positions. In contrast, the glucopyranosyl residues of the S-laminaribioside and gentiobiose and S-cellobioside and sophorose moieties occupy subsite +1 that is located between the Trp286 and Trp434 residues. In the case of the S-laminaribioside and gentiobiose moieties, the apolar face of the glucopyranosyl residue at subsite +1 is geometrically complementary with the pyrrole ring of Trp286, while the polar face of the glucopyranosyl residue positions itself over the phenyl ring of Trp434. In the S-cellobioside and sophorose moieties, the polar and the apolar faces of glucopyranosyl residue at subsite +1 are in contact with the pyrrole ring of Trp286 and the phenyl ring of Trp434, respectively. That is, the four positional sugar isomers can adopt two different orientations with respect to the phenyl/pyrrole rings of Trp286 or Trp434. Thus, it follows that if a substrate binds to the broad specificity β-D-glucan glucohydrolase, substrate binding will be largely independent of polysaccharide conformation and the glycosidic linkage positions between adjacent non-reducing-end β-D-glucosyl residues, hence explaining why the β-D-glucan glucohydrolases have broad substrate specificities.

The crystallographic observations for the family GH3 β-D-glucan glucohydrolase in complex with substrate thio-analogues contrast with the conformational constraints imposed on substrates for family GH1 (1→4)-β-D-glucan glucohydrolases,[21,22] which must have the correct conformation to bind multiple glucosyl residues to the active site, which is found at the bottom of a much deeper, narrower funnel. The depth and narrow nature of the active site tunnel in the GH1 β-D-glucosidases impose considerably greater geometrical constraints on substrates that will fit into the active site, and hence tighten the substrate specificities of these enzymes. Thus, family GH3 and family GH1 enzymes represent a contrasting pair of polysaccharide *exo*-hydrolases with broad and relatively tight substrate specificities, respectively.

## 4. Catalytic mechanism and domain movements during catalysis

Now that we could explain the molecular bases for substrate binding and substrate specificity of the barley β-D-

glucan glucohydrolase, it was possible to examine the atomic details of catalysis, given the fact that the enzyme possesses *exo*-hydrolytic and retaining (e→e) mechanisms of action.[7,15] There have been a number of excellent recent reviews[24,39–41] on the mechanisms of catalysis of glycosyl hydrolases. Hydrolysis of glycosidic linkages by glycosyl hydrolases is usually effected through two catalytic residues. One is a general acid catalyst, which donates the proton required for hydrolysis, and the other acts like a general base catalyst; it is commonly called a catalytic nucleophile in retaining hydrolases, and a catalytic base in inverting hydrolases.[39–41] Oxocarbenium ion-like transition states are generally formed during the hydrolytic reactions, and depending on the spatial disposition of the two catalytic residues, anomeric configuration of hydrolysis products will be retained or inverted during hydrolysis.[39–41]

In the barley β-D-glucan glucohydrolase, as with other family GH3 plant enzymes, the catalytic nucleophile amino acid residue (D) is located in a highly conserved GFVIS*D*W sequence motif, and is surrounded by a landscape of amino acid residues with characteristics similar to those in other family GH3 enzymes.[16,27] Molecular modelling and hydrophobic cluster analyses indicate that the catalytic nucleophile in plant GH3 family enzymes is always found near the COOH-terminus of β-strand g in the first domain,[1] and that this β-strand is always positioned in the shallow active site pocket that is located at the interface of the two domains.[27] Labelling the barley β-D-glucan glucohydrolase with conduritol B epoxide or 2,4-dinitrophenyl 2-deoxy-2-fluoro-β-D-glucopyranoside, coupled with comparative tryptic peptide mapping and other structural analyses, shows that Asp285 is the catalytic nucleophile (PDB accession codes 1IEV and 1IEW).[27] The structure of the cyclohexitol–enzyme complex has been solved to 2.80 Å resolution, and as shown in the difference Fourier electron density map of the active site (Fig. 4), the C1 of the cyclohexitol ring is placed 1.33 Å from the Oδ1Asp285, indicative of a covalent bond between these two atoms. The covalent linkage is axial to the plane of the cyclohexitol ring and is therefore equivalent to an α-anomeric linkage for D-glucosides.[27] Furthermore, molecular modelling showed that amino acid residue Asp285 of the barley enzyme, or its equivalent in other enzymes, is invariant in all family GH3 glycoside hydrolases and is likely to be the catalytic nucleophile.[1,2] To this end, Asp12 in a 13.2 kDa β-D-glucosidase fragment isolated from *Aspergillus wentii* was previously identified as a catalytic nucleophile in the pioneering work of Günter Legler.[42] Further, Asp242 in the *N*-acetyl-β-D-glucosaminidase from *Vibrio furnisii*,[43] Asp261 in the β-D-glucosidase from *Aspergillus niger*,[44] Asp247 in the β-D-glucosidase from *Flavobacterium meningosepticum*,[45] Asp223 in the glucosylceraminidase from *Paenibacillus* sp. TS12,[46] and Asp283 in the bifunctional β-*N*-acetyl-D-glucosaminidase/β-D-glucosidase from *Cellulomonas fimi*,[47] all equivalent to Asp285 in the barley enzyme, have been identified experimentally as catalytic nucleophiles.

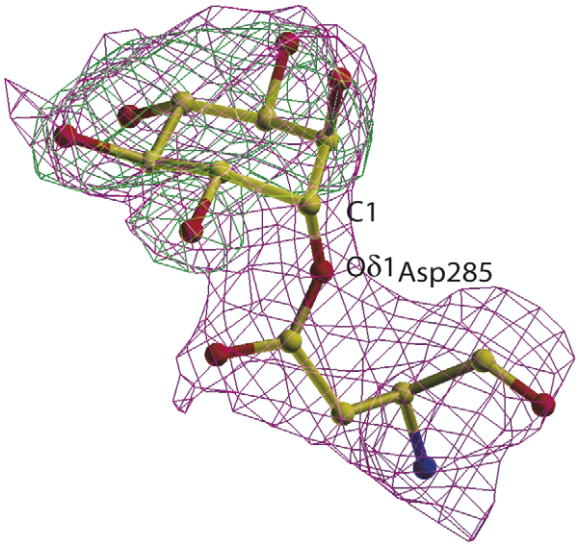


**Figure 4.** Electron density map of the covalently linked cyclohexitol ring and Oδ1Asp285 in the active site of β-D-glucan glucohydrolase. The C1 of the cyclohexitol ring and Oδ1Asp285 are separated by 1.33 Å. The derived $2|F_o| - |F_c|$ and $|F_o| - |F_c|$ Fourier syntheses are contoured at 1.2σ (magenta) and 3σ (green), respectively. $F_o$ and $F_c$ are the observed and calculated structure factors, respectively. Adapted with permission from Elsevier Science.[27]

The identification of the catalytic acid/base, using biochemical methods such as chemical labelling, is not straightforward and in many cases the identity of the catalytic acid/base has been deduced from structural information in combination with bioinformatics.[1,2] From the 3D structure of the β-D-glucan glucohydrolase it became obvious that the Asp285 residue lies within 3.0 Å of the C1 of the glucose molecule that is bound to the enzyme in subsite −1 of the substrate binding pocket.[26,27] Three other acidic residues, Asp95, Glu220 and Glu491, are also located near the C1 of the bound glucose. However, the atomic distances and relative dispositions immediately suggest that Glu491 is the most likely candidate for the catalytic acid/base.[26,27] This was confirmed experimentally with a non-hydrolysable S-glycosyl substrate analogue, $4^{I}$, $4^{III}$, $4^{V}$-S-trithiocellohexaose,[27] which was diffused into the enzyme crystals. The likely catalytic acid/base Glu491 was deduced from the distances between the S-atom of the S-glycosidic linkage and conserved amino acid residues at the catalytic site. The catalytic acid/base in the barley enzyme Glu491 was present only in closely-related members of the GH3 family. It then logically followed that if Glu491 is variant in the family GH3 glycoside hydrolases, then the role of the catalytic acid/base could be adopted by equivalently positioned amino acid residues in more distant members of the GH3 family.[1,2,4]

Transition-state mimics have been used extensively to study putative substrate transition states and the mechanistic aspects of oligo- and polysaccharide distortions by glycosyl hydrolases.[39,48–52] The binding of the two transition-state mimics phenyl gluco-imidazole (PheGlcIm) and anilinomethyl gluco-imidazole (AmGlcIm), which are useful chemical tools for mimicking transition states of glycoside hydrolases, were investigated with the β-D-glucan glucohydrolase by X-ray crystallography (Figs. 5 and 6) and by ab initio quantum mechanical modelling.[53,54] These inhibitors belong to the C(2)-substituted *gluco*-configured tetrahydroimidazopyridine family that possess a non-hydrolysable glycosidic C–N bond between the C10 and the N1 atom of the 'sugar' and imidazole moieties, and their anomeric carbons are $sp^2$-hybridized and double-bonded with the exocyclic N1 atoms.[39,55]

The binding of AmGlcIm with the β-D-glucan glucohydrolase proceeds with a $K_i$ constant of 0.6 nM and shows that in the AmGlcIm–enzyme complex an additional residue, Tyr253, which has not been seen previously in interactions with mechanism-based inhibitors, and a new water molecule are positioned between subsites −1 and +1, and are recruited for AmGlcIm binding. Analysis of the AmGlcIm–enzyme binary complex (PDB accession code 1X39) reveals that an intricate network of hydrogen bonds exists between the enzyme's active site residues and that the gluco-imidazole is shorter by approximately 0.2–0.5 Å, compared with distances of hydrogen bonds in the Michaelis complex.[27,53,54] The 'glucose' moiety of the gluco-imidazoles adopts a $^4E$ conformation (Figs. 5 and 6) that is vital for the low nanomolar binding, and the N1 atom of the AmGlcIm is positioned optimally for in-line protonation by the Oε1 atom of the catalytic acid/base Glu491.[53,54] Further, it was deduced that the enzyme derives binding energies from both glycone and aglycone components of the gluco-imidazole. Finally, quantum mechanical

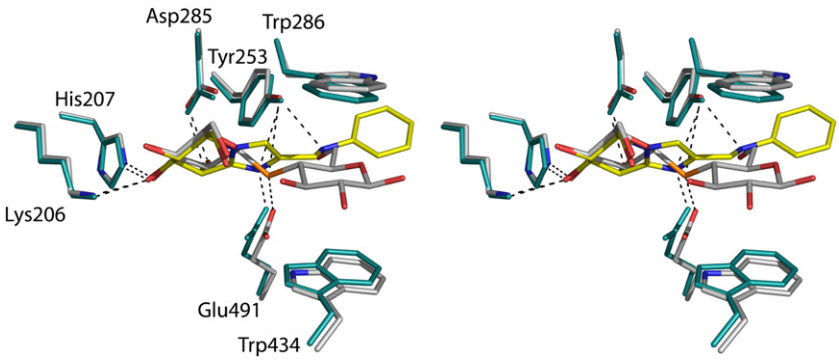


**Figure 5.** The enzyme–AmGlcIm complex is superposed over the enzyme–S-cellobioside moiety complex. The S-cellobioside moiety is coloured grey (carbons), orange (sulfur) and red (oxygens), and the interacting residues are in grey (carbons), blue (nitrogens) and red (oxygens). The colour coding of the AmGlcIm complex is in yellow (carbons), blue (nitrogens) and red (oxygens), and the interacting residues are colour coded as specified above. The five separations (dashed lines) between Lys206, His207, Tyr253, Asp285 and Glu491 are shown; they are 0.17–0.53 Å shorter than in the enzyme–S-cellobioside moiety complex. The two structures were superposed over the Cα atoms of the residues 1-602, with a rmsd value of 0.392 Å. Adapted with permission from the American Chemical Society.[54]

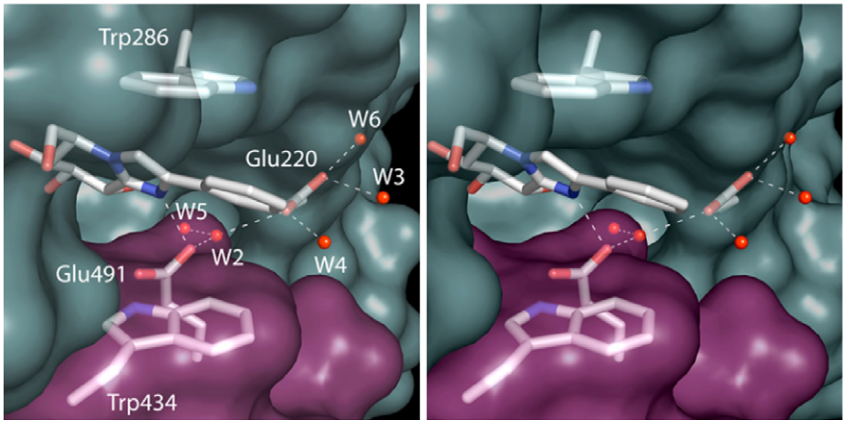


**Figure 6.** Stereo representation of the water channel involved in the hydrolytic cycle of the barley β-D-glucan glucohydrolase. The four amino acid residues Glu491, Glu220, Trp286 and Trp434 and the PheGlcIm inhibitor molecule are presented as sticks and atoms are coloured grey (carbons), blue (nitrogens) and red (oxygens). The five water molecules (W2–W6) shown as red spheres are connected with each other, and with Glu491 and Glu220 through several hydrogen bonding interactions (marked by white dashed lines), and are directed to the N1 atom of the tetrahydroimidazopyridine moiety that mimics glycosidic oxygen. Adapted with permission from the American Chemical Society.[54]

modelling, based on the structural data, predicts that protons could be positioned on the N1 atoms of the gluco-imidazole, and that the catalytic acid/base Glu491 could carry an overall negative charge.[54]

In another β-D-glucan glucohydrolase complex with the transition-state mimic PheGlcIm (PDB accession codes 1LQ2 and 1X38), seven water molecules have been identified in the active site,[53,54] from which five water molecules are associated with the catalytic acid/base Glu491 and with another acidic residue Glu220 (Fig. 6). These two residues are highly conserved in the GH3 family of hydrolases,[1,2] and while the former residue serves as the catalytic acid/base, the latter residue probably plays a role in coordinating the water molecules around the acid/base catalyst.[27,53,54] It was further suggested that these two acidic amino acids cooperate with Arg291 and guide the associated water molecules to their target location during hydrolysis (Fig. 6). At least four of the solvent molecules are highly conserved in their positions and have previously been observed in the 2-deoxy-2-fluoro-α-gluco-pyranosyl- and PheGlcIm-β-D-glucan glucohydrolase complexes.[27,53,54]

The key message that emerges from the crystallographic analyses of the PheGlcIm– and AmGlcIm–β-D-glucan glucohydrolase complexes is that during transition-state development and substrate distortion, amino acid residues from both the −1 and +1 subsites participate, but with significantly different roles.[54] These considerations could be important for the design of highly efficient transition-state mimics for inhibiting the barley β-D-glucan glucohydrolase and other enzymes, whereby the enzyme could harness binding energy from the aglycone portions of improved transition-state mimics at the +1 subsite. It would be expected that local active site geometry would play a key role during these interactions, because no binding was observed between +1 subsite-positioned amino acid residues of a family GH1 β-D-glucosidase and the appended functional groups of a series of 18 transition-state mimics.[56]

From the comparative analyses of the two transition-state-enzyme complexes,[54] one would predict that domain movements will be important during catalysis. This possibility can be explored by analyzing rigid body correlated motions[54] of the two independent domains of the β-D-glucan glucohydrolase,[57–59] rather than simply analyzing conformational fluctuations of individual parts or local regions of the enzyme molecule.[60] From the initial structure of the β-D-glucan glucohydrolase enzyme it was suggested that the 16 amino acid residue helix-like linker that connects the two domains could act as a molecular hinge in a spring- or stretch-like fashion; this movement would allow the two domains to move relative to each other. The possibility that precisely this type of domain motion could take place during catalysis was shown in the 3D structural analyses of the β-D-glucan glucohydrolase in complex with the two transition-state mimics AmGlcIm and PheGlcIm.[54] The high resolution data of these two complexes defined the fine details of rigid body motions of the two independent domains of the enzyme.[58,59] It was observed in AmGlcIm– and PheGlcIm–enzyme complexes that librational motion L tensors of domains 1 and 2 were at least one order of magnitude higher than those of translational motion T and screw motion S tensors. We concluded that L motion tensors showed anisotropy and that the two T and S tensors were less anisotropic, which indicated that translational and screw motions of the domains 1 and 2 were limited. This mutual librational movement of both domains was also observed in a high resolution structure of the β-D-glucan glucohydrolase with bound glucose, in which the librational L tensor values had marginally but significantly higher values compared with values observed in the AmGlcIm– and PheGlcIm–enzyme complexes (Hrmova, M.; Streltsov, V.; Fincher, G. B.; Varghese, J. N., unpublished data). Thus, it could be concluded that libration is the prevalent type of motion linking the two domains of the β-D-glucan glucohydrolase, and that this motion could play a significant role during induced fit closure of the active site during catalysis or inhibitor binding. Because the two catalytic residues Asp285 and Glu491 are located on the two separate domains, it can be envisaged that the two domains move towards and away from each other during the reaction sequence, as the enzyme goes through successive catalytic events.

## 5. Concluding remarks

Glycoside hydrolases play key roles in a wide range of biological processes. Crystal structures of the barley β-D-glucan glucohydrolase, obtained from both native enzyme and from the enzyme in complex with a substrate analogues and mechanism-based inhibitors, have enabled the basis of substrate specificity, the mechanism of catalysis, and the role of domain movements during the catalytic cycle to be defined at atomic levels. The propensity of the enzyme to hydrolyze a broad range of substrates with (1→2)-, (1→3)-, (1→4)- and (1→6)-β-D-glucosidic linkages can be rationalized from crystal structures of the enzyme in complex with non-hydrolysable S-glycoside substrate analogues, and from molecular modelling. The glucose product of the reaction, which is released from the non-reducing termini of substrates, remains bound to the β-D-glucan glucohydrolase in the −1 subsite of the active site, until a new substrate molecule approaches the enzyme. If dissociation of the glucose from the enzyme active site could be synchronized throughout the crystal, time-resolved Laue X-ray crystallography could be applied to follow the conformational changes of the enzyme that occur as the glu-

cose product diffuses away and the incoming substrate is bound. The analyses of the ligand–enzyme interactions involved in binding of inhibitors, substrate analogues and transition-state mimics could suggest potentially novel organo-synthetic avenues for future improvements in inhibitor design. These considerations could be important, for example in design of highly efficient tailored-made inhibitors of the plant β-retaining glycoside hydrolases, which could control vital biological events in life cycles of economically important plants or in certain situations as herbicides.

## Acknowledgements

This work was supported by grants from the Australian Research Council (to G.B.F. and M.H.), the Grains Research and Development Corporation (to G.B.F.), the Australian Synchrotron Research Programme (to M.H.) and the Australian Partnership for Advanced Computing Facility (to M.H.). We thank Drs. Jose Varghese, Victor Streltsov, Ross De Gori and Alys Peisley (CSIRO-MHT, Melbourne, Australia), Professor Andrea Vasella (ETH-Hönggerberg, Zürich, Switzerland), Dr. Brian Smith (WEHI, Melbourne, Australia) and Drs. Hugues Driguez and Sebastien Fort (CNRS-CERMAV, Grenoble, France) for stimulating collaboration and advice. Contributions from Professor Keith Moffat and Dr. Vukica Srajer (APS, Chicago, USA) are also acknowledged. The support of the Australian Synchrotron Research Programme (to M.H., Victor Streltsov and Jose Varghese), which is funded by the Commonwealth of Australia under the Major National Research Facilities Programme, is also gratefully acknowledged.

## References

1. Coutinho, P.; Henrissat, B. In *Recent Advances in Carbohydrate Bioengineering*; Gilbert, H., Davies, G., Henrissat, B., Svensson, B., Eds.; The Royal Society of Chemistry: Cambridge, 1999; pp 3–12.
2. Harvey, A. J.; Hrmova, M.; De Gori, R.; Varghese, J. N.; Fincher, G. B. *Proteins Struct. Funct. Genet.* **2000**, *41*, 257–269.
3. Rojas, A. L.; Fischer, H.; Eneiskaya, E. V.; Kulminskaya, A. A.; Shabalin, K. A.; Neustroev, K. N.; Craievich, A. F.; Golubev, A. M.; Polikarpov, I. *Biochemistry* **2005**, *44*, 15578–15584.
4. Cournoyer, B.; Faure, D. *J. Mol. Microbiol. Biotechnol.* **2003**, *5*, 190–198.
5. Hrmova, M.; Fincher, G. B. *Plant Mol. Biol.* **2001**, *47*, 73–91.
6. Takeda, H.; Yoshikawa, T.; Liu, X.-Z.; Nakagawa, N.; Li, Y.-Q.; Sakurai, N. *Plant Cell Physiol.* **2004**, 436–444.
7. Hrmova, M.; Harvey, A. J.; Wang, J.; Shirley, N. J.; Jones, G. P.; Høj, P. B.; Fincher, G. B. *J. Biol. Chem.* **1996**, *271*, 5277–5286.
8. Hrmova, M.; Fincher, G. B. *Plant Physiol.* **2001**, *125*, 54–57.
9. Harvey, A. J.; Hrmova, M.; Fincher, G. B. *Physiol. Plant.* **2001**, *113*, 108–120.
10. Kotake, T.; Nagawa, N.; Takeda, K.; Sakurai, N. *Plant Cell Physiol.* **1997**, *38*, 194–200.
11. Labrador, E.; Nevins, D. J. *Physiol. Plant.* **1989**, *77*, 479–486.
12. Kim, J. B.; Olek, A. T.; Carpita, N. C. *Plant Physiol.* **2000**, *123*, 471–485.
13. Cline, K.; Albersheim, P. *Plant Physiol.* **1981**, *68*, 207–220.
14. Crombie, H.; Chengappa, S.; Hellyer, A.; Reid, J. S. G. *Plant J.* **1998**, *15*, 27–38.
15. Hrmova, M.; Fincher, G. B. *Carbohydr. Res.* **1998**, *305*, 209–221.
16. Hrmova, M.; De Gori, R.; Smith, B. J.; Driguez, H.; Varghese, J. N.; Fincher, G. B. *Plant Cell* **2002**, *14*, 1033–1052.
17. Murray, P.; Aro, N.; Collins, C.; Grassick, A.; Penttila, M.; Saloheimo, M.; Tuohy, M. *Protein Express. Purif.* **2004**, *38*, 248–257.
18. Kawai, R.; Igarashi, K.; Kitaoka, M.; Ishii, T.; Samejima, M. *Carbohydr. Res.* **2004**, *339*, 2851–2857.
19. Seidle, H. F.; Huber, R. E. *Arch. Biochem. Biophys.* **2005**, 254–264.
20. Sinnott, M. L. *Chem Rev.* **1990**, *90*, 1171–1202.
21. Barrett, T.; Suresh, C. G.; Tolley, S. P.; Dodson, E. J.; Hughes, M. A. *Struct. Fold. Des.* **1995**, *3*, 951–960.
22. Burmeister, W. P.; Cottaz, S.; Driguez, H.; Iori, R.; Palmieri, S.; Henrissat, B. *Struct. Fold. Des.* **1997**, *5*, 663–675.
23. Taylor, L. E., II; Henrissat, B.; Coutinho, P. M.; Ekborg, N. A.; Howard, M. B.; Hutcheson, S. W.; Weiner, R. M. *J. Bacteriol.* **2006**, *188*, 3849–3861.
24. Davies, G. J.; Gloster, T. M.; Henrissat, B. *Curr. Opp. Struct. Biol.* **2005**, *15*, 637–645.
25. Hrmova, M.; Varghese, J. N.; Høj, P. B.; Fincher, G. B. *Acta Crystallogr. Sect., D* **1998**, *54*, 1687–1689.
26. Varghese, J. N.; Hrmova, M.; Fincher, G. B. *Struct. Fold. Des.* **1999**, *7*, 179–190.
27. Hrmova, M.; Varghese, J. N.; De Gori, R.; Smith, B.; Driguez, H.; Fincher, G. B. *Struct. Fold. Des.* **2001**, *9*, 1005–1016.
28. Davies, G.; Henrissat, B. *Struct. Fold. Des.* **1995**, *7*, 853–859.
29. Moffat, K. *Methods Enzymol.* **1997**, *277*, 433–447.
30. Stoddard, B. L. *Methods* **2001**, *24*, 126–138.
31. Lee, R. C.; Hrmova, M.; Burton, R. A.; Lahnstein, J.; Fincher, G. B. *J. Biol. Chem.* **2003**, *278*, 5377–5387.
32. Zou, J. Y.; Kleywegt, G. J.; Stahlberg, J.; Driguez, H.; Nerinckx, W.; Claeyssens, M.; Koivula, A.; Teeri, T. T.; Jones, T. A. *Struct. Fold. Des.* **1999**, *7*, 1035–1045.
33. Sidhu, G.; Withers, S. G.; Nguyen, N. T.; McIntosh, L. P.; Ziser, L.; Brayer, G. D. *Biochemistry* **1999**, *38*, 5346–5354.
34. Davies, G. J.; Mackenzie, L.; Varrot, A.; Dauter, M.; Brzozowski, A. M.; Schülein, M.; Withers, S. G. *Biochemistry* **1998**, *37*, 11707–11713.
35. Sulzenbacher, G.; Driguez, H.; Henrissat, B.; Schülein, M.; Davies, G. J. *Biochemistry* **1996**, *35*, 15280–15287.
36. Tews, I.; Perrakis, A.; Oppenheim, A.; Dauter, Z.; Wilson, K. S.; Vorgias, C. E. *Nat. Struct. Biol.* **1996**, *3*, 638–648.
37. Ikegami, M.; Sato, T.; Suzuki, K.; Noguchi, K.; Okuyama, K.; Kitamura, S.; Takeo, K.; Ohno, S. *Carbohydr. Res.* **1995**, *271*, 137–150.
38. Rohrer, D. C.; Sarko, A.; Bluhm, T. L.; Lee, Y. N. *Acta Crystallogr., Sect. B* **1980**, *36*, 650–654.

39. Vasella, A. T.; Davies, G. J.; Böhm, M. *Curr. Opin. Chem. Biol.* **2002**, *6*, 619–629.
40. Lairson, L. L.; Withers, S. G. *Chem. Commun.* **2004**, 2243–2248.
41. Koshland, D. E., Jr. *Biol. Rev.* **1953**, *28*, 416–436.
42. Bause, E.; Legler, G. *Biochim. Biophys. Acta* **1980**, *626*, 459–465.
43. Vocadlo, D. J.; Mayer, C.; He, S.; Withers, S. G. *Biochemistry* **2000**, *39*, 117–126.
44. Dan, S.; Marton, I.; Dekel, M.; Bravdo, B.-A.; He, S.; Withers, S. G.; Shoseyov, S. G. *J. Biol. Chem.* **2000**, *275*, 4973–4980.
45. Chir, J.; Withers, S.; Wan, C.-F.; Li, Y.-K. *Biochem. J.* **2002**, *365*, 857–863.
46. Paal, K.; Ito, M.; Withers, S. G. *Biochem. J.* **2004**, *378*, 141–149.
47. Mayer, C.; Vocadlo, D. J.; Mah, M.; Rupitz, K.; Stoll, D.; Warren, R. A. J.; Withers, S. G. *FEBS J.* **2006**, *273*, 2929–2941.
48. Heightman, T. D.; Vasella, A. T. *Angew. Chem., Int. Ed.* **1999**, *38*, 750–770.
49. Zechel, D. L.; Withers, S. G. *Acc. Chem. Res.* **2000**, *33*, 11–18.
50. Varrot, A.; Schülein, M.; Pipelier, M.; Vasella, A.; Davies, G. J. *J. Am. Chem. Soc.* **1999**, *121*, 2621–2622.
51. Varrot, A.; Tarling, C. A.; Macdonald, J. M.; Stick, R. V.; Zechel, D. L.; Withers, S. G.; Davies, G. J. *J. Am. Chem. Soc.* **2003**, *25*, 7496–7497.
52. Notenboom, V.; Williams, S. J.; Hoos, R.; Withers, S. G.; Rose, D. R. *Biochemistry* **2000**, *39*, 11553–11563.
53. Hrmova, M.; De Gori, R.; Smith, B. J.; Vasella, A.; Varghese, J. N.; Fincher, G. B. *J. Biol. Chem.* **2004**, *279*, 4970–4980.
54. Hrmova, M.; Streltsov, V. A.; Smith, B. J.; Vasella, A.; Varghese, J. N.; Fincher, G. B. *Biochemistry* **2005**, *44*, 16529–16539.
55. Terinek, M.; Vasella, A. *Helv. Chim. Acta* **2004**, *87*, 3035–3049.
56. Gloster, T. M.; Meloncelli, P.; Stick, R. V.; Zechel, Z.; Vasella, A.; Davies, G. J. *J. Am. Chem. Soc.* **2007**, *129*, 2345–2354.
57. Winn, M. D.; Isupov, M. N.; Murshudov, G. N. *Acta Crystallogr., Sect. D* **2001**, *57*, 122–133.
58. Yousef, M. S.; Fabiola, F.; Gattis, J. L.; Somasundaram, T.; Chapman, M. S. *Acta Crystallogr., Sect. D* **2002**, *58*, 2009–2017.
59. Painter, J.; Merritt, E. A. *Acta Crystallogr., Sect. D* **2005**, *61*, 465–471.
60. Antoniou, D.; Basner, J.; Nunez, S.; Schwartz, S. D. *Chem. Rev.* **2006**, *106*, 3170–3187.